Yttrium Doping Stabilizes the Structure of $Ni_3(NO_3)_2(OH)_4$ Cathodes for Application in Advanced Ni-Zn Batteries

Xinyu Feng [a], Siwen Zhang [a], Jiazhuo Li [a], Yingfang Hu [a], Rongyuan Ge [a], Yaowen Shi [a], Yali Yao [b], Bosi Yin [a,*] and Tianyi Ma [c,*]

The energy density (E, Wh/kg) and power density (P, W/kg) of the devices were calculated using the following formula:

$$E = \int IVdt/m \quad (1)$$

$$P = E/\Delta t \quad (2)$$

Where I was the discharging current, V was the discharging voltage, dt was the time differential, m was the total mass of the active electrode materials, Δt was the discharging time.

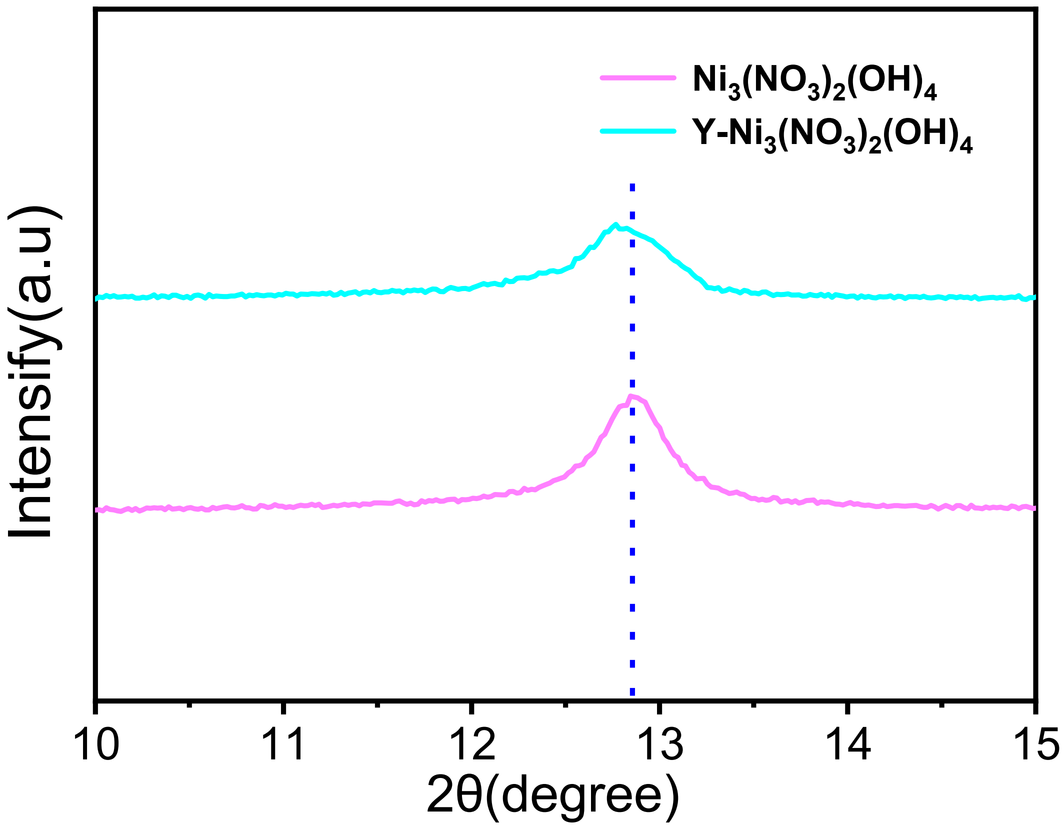

Figure S1. Part of the XRD patterns of $Ni_3(NO_3)_2(OH)_4$ and $Y\text{-}Ni_3(NO_3)_2(OH)_4$.

Materials	Y(at%)	Ni(at%)	Y:Ni
$Y\text{-}Ni_3(NO_3)_2(OH)_4$	2.41	31.73	7.59%

Table 1. Determine the atomic ratio of Y to Ni in $Y\text{-}Ni_3(NO_3)_2(OH)_4$ by EDS.

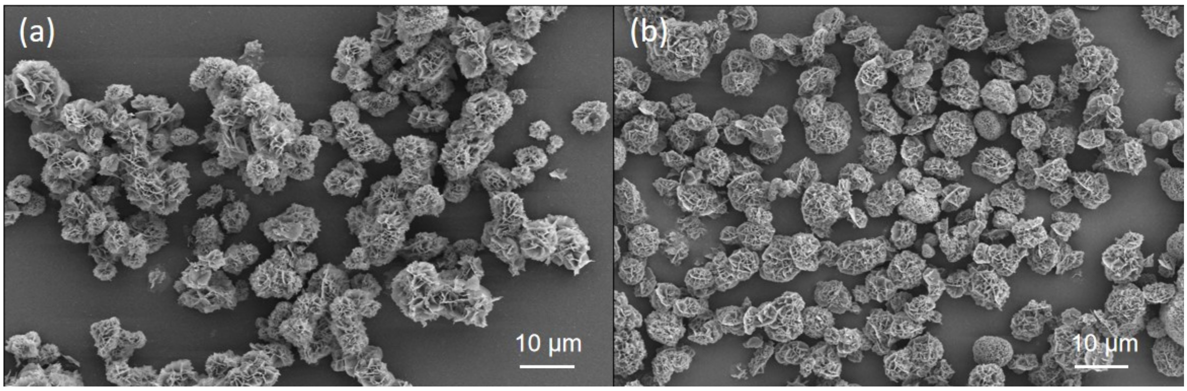

Figure S2. (a) SEM images of $Ni_3(NO_3)_2(OH)_4$, (b)SEM images of Y-$Ni_3(NO_3)_2(OH)_4$.

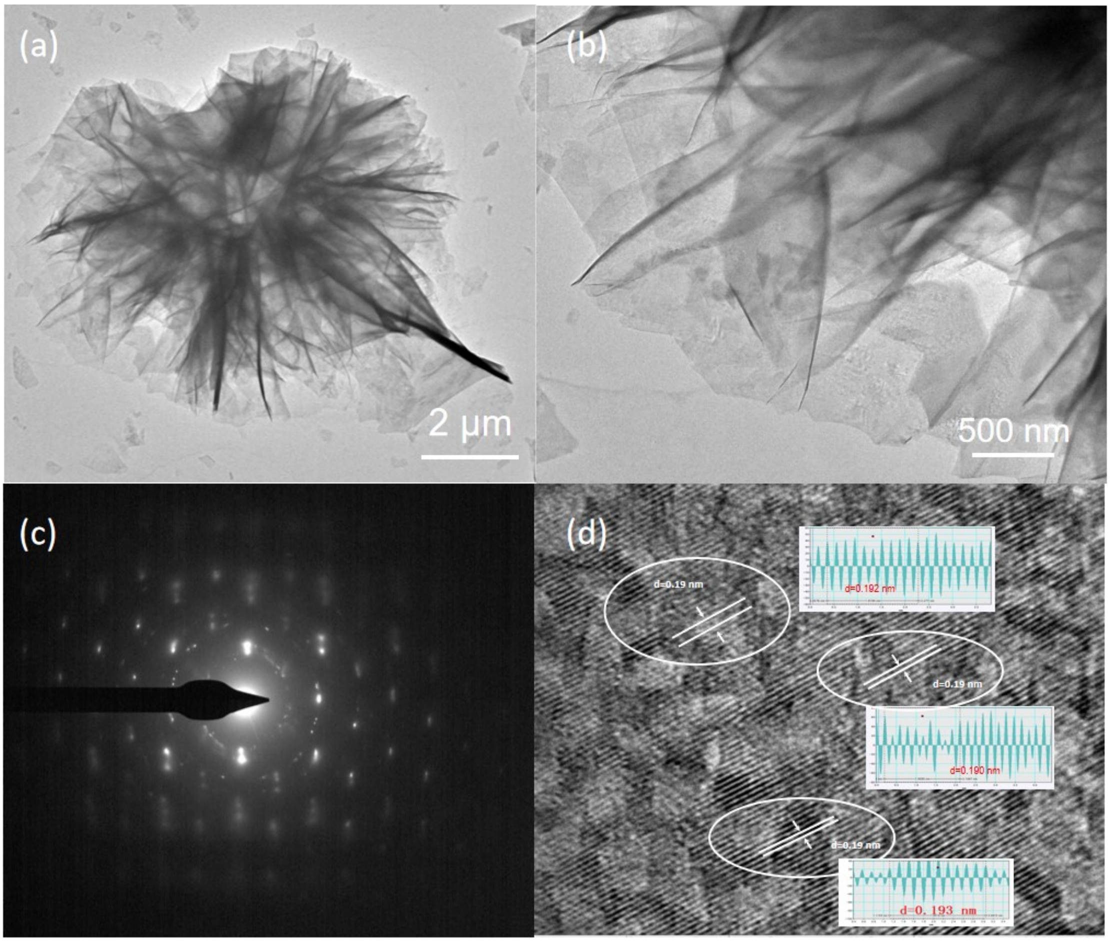

Figure S3. (a-b)TEM images of $Ni_3(NO_3)_2(OH)_4$, (c)SAED pattern of $Ni_3(NO_3)_2(OH)_4$, (d) HRTEM of $Ni_3(NO_3)_2(OH)_4$.

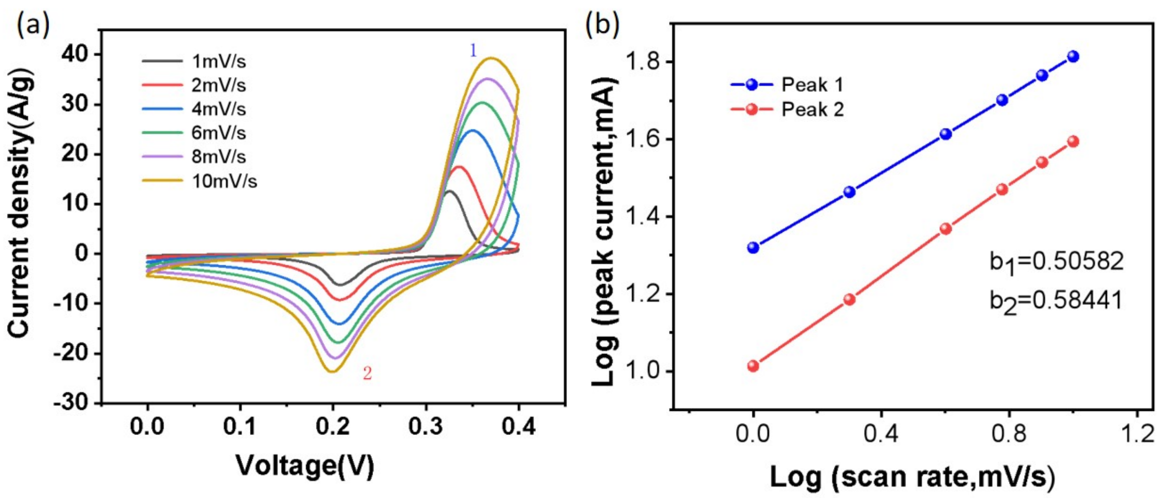

Figure S4. (a) CV curves of the Y-$Ni_3(NO_3)_2(OH)_4$ electrodes at different scan rates, (b) Relationship of Y-$Ni_3(NO_3)_2(OH)_4$ between log (*i*) and log (*v*).

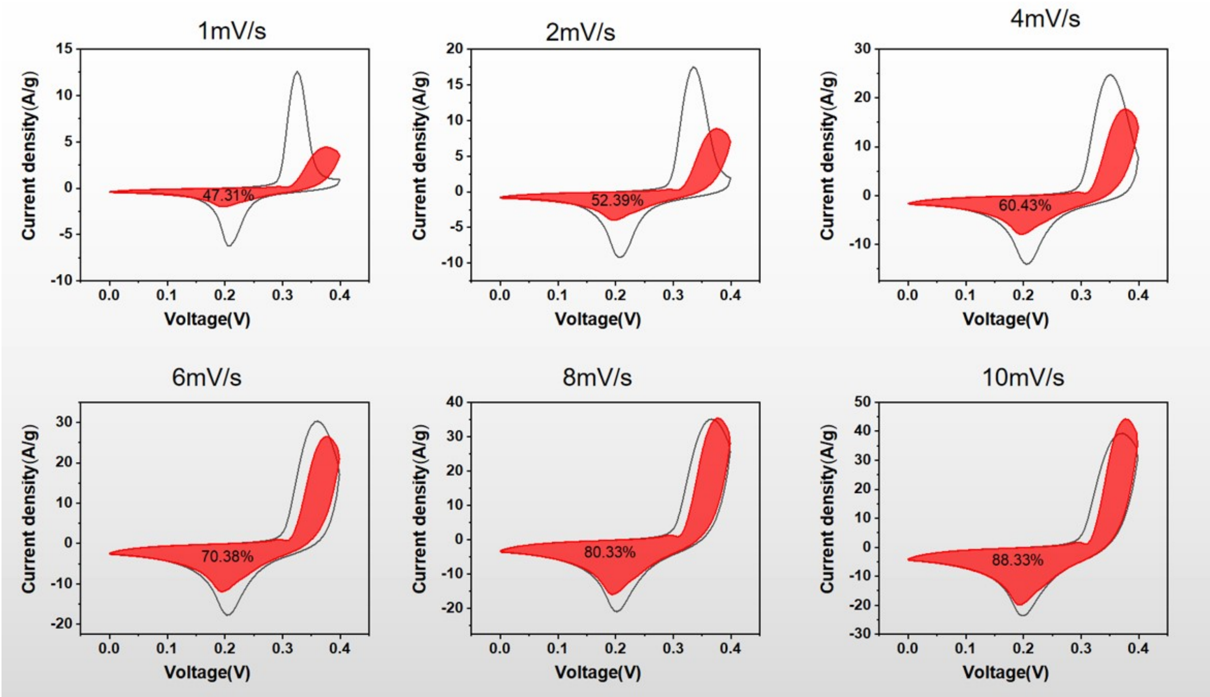

Figure S5. Capacitive contributions of $Ni_3(NO_3)_2(OH)_4$ at different scan rates.

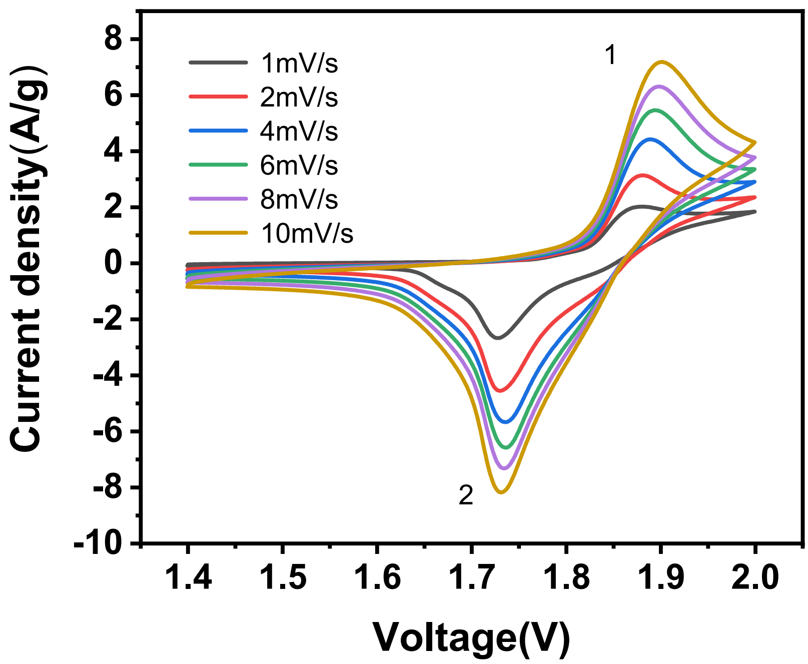

Figure S6. CV curves of the $Ni_3(NO_3)_2(OH)_4$//Zn battery electrodes at different scan rates.

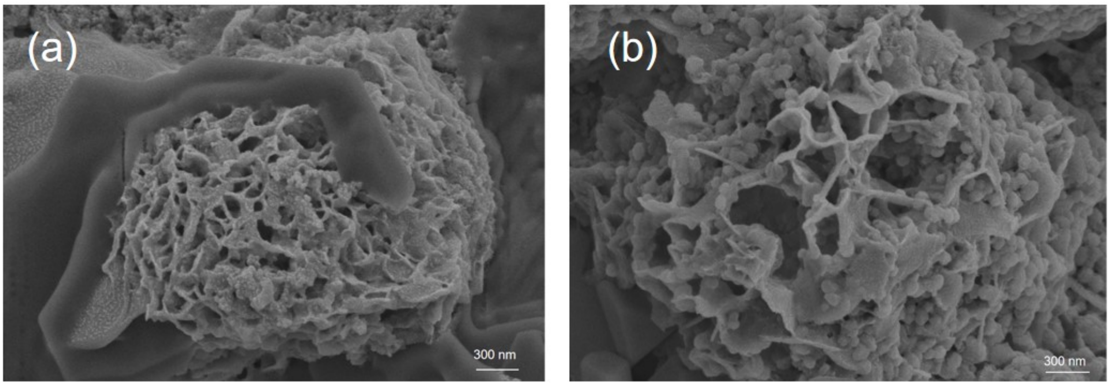

Figure S7. SEM of Y-$Ni_3(NO_3)_2(OH)_4$ after 100 charge-discharge cycles at 1 A/g.

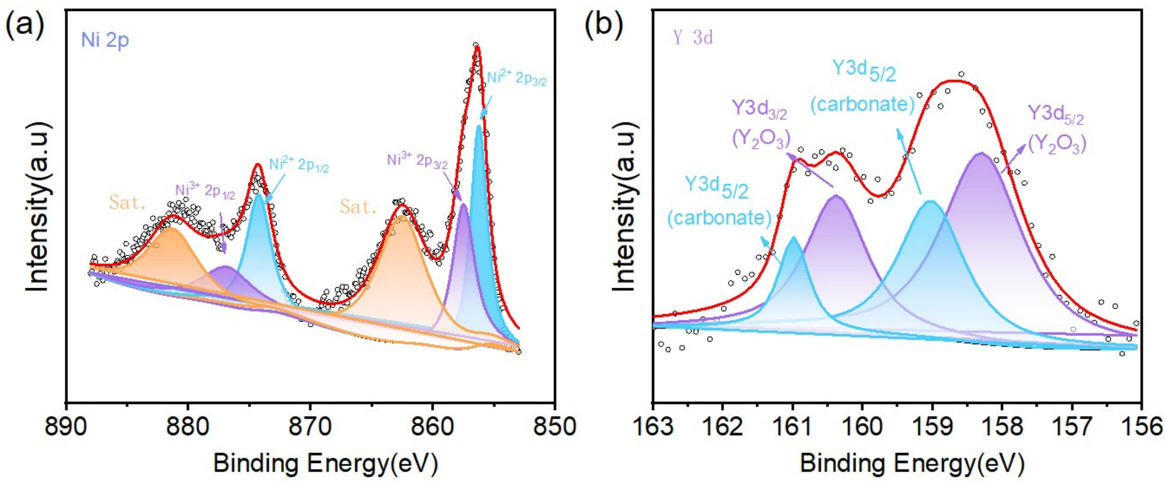

Figure S8. XPS of Y-$Ni_3(NO_3)_2(OH)_4$ after 100 charge-discharge cycles at 1 A/g.